Chemical Physics Letters 477 (2009) 281–284

Contents lists available at ScienceDirect

Chemical Physics Letters

journal homepage: www.elsevier.com/locate/cplett

Puzzling spectral structures of molecular vibration observed in ultrafast pump–probe experiment of transparent material

A. Ozawa [a,*], T. Kobayashi [a,b,c,d,e]

[a] Department of Physics, Graduate School of Science, The University of Tokyo, 7-3-1 Hongo, Bunkyo, Tokyo 113-0033, Japan
[b] ICORP, JST, 4-1-8 Honcho, Kawaguchi, Saitama 332-0012, Japan
[c] National Chiao-Tung University, Hsinchu 300, Taiwan
[d] University of Electro-Communications, 1-5-1 Chofugaoka, Chofu 182-8585, Japan
[e] Osaka University, 2-6 Yamada-oka, Suita, Osaka 565-0971, Japan

ARTICLE INFO

Article history:
Received 13 April 2009
In final form 30 June 2009
Available online 3 July 2009

ABSTRACT

A sub-5-fs ultrafast pump–probe experiment was applied to neat liquid tetrahydrofuran (THF). The observed periodic modulation of transmittance change (ΔT), $\sim 5 \times 10^{-3}$, is assigned to the ground-state vibrational mode of C–H stretching. Although the sample has no stationary absorption in the wavelength region under study, the modulation amplitude shows strong dependence on the probe photon energy. A model is proposed to explain this feature based on the coherent Raman coupling between the fundamental and Stokes-shifted spectral components. The results demonstrate that a special attention is required in distinguishing the ground- and excited-state vibrational signals in ultrafast transient absorption spectroscopy.

1. Introduction

Recent improvements in femtosecond pulsed lasers have enabled detailed real-time investigation of high-frequency vibrational processes and ultrafast electronic relaxations [1–6]. The use of impulsive stimulated Raman scattering (ISRS) has been proposed and investigated in a pump–probe setup [7–14]. In these experiments, pump pulses produce wave packets in the ground-state due to the ISRS process and the intensity modulations of subsequent probe pulses are detected for different delay times.

In ultrafast transient absorption spectroscopy using the pump–probe setup, it is sometimes essential, but often difficult, to distinguish the excited-state vibrational modes from the ground-state ones; several methods have been proposed to identify the origin of the signals in terms of wave packets in either the ground state or excited states. Based on a simple model that the vibrational harmonic potential in the excited state is shifted from that of in the ground state, the initial phase of the modulation is expected to be sinusoidal and cosinusoidal for the ground- and excited-state vibrations, respectively [15,16]. Though the derivation of information on the initial phase is a benefit of real-time observation, it is sometimes difficult to precisely determine the initial phase because of the complex mixing of the sinusoidal and cosinusoidal phases or the presence of some unspecified artifacts at the zero-delay time.

Since the ground-state wave packets modulate the induced absorption from the ground state, the signals of quantum beats due to the wave packets in the ground state are expected to appear only in the spectral region where there is stationary absorption or stimulated emission. In addition to this conventional understanding, our previous report has revealed that the ground-state vibration modulates the spectral region lower than the absorption edge. This energy region is separated from the absorption edge by the vibrational energy [9]. In a transparent medium, the effect of electronic transition is negligible and the ground-state vibrational modes are induced through ISRS using pump pulses.

In the present Letter, we report on our theoretical model and our experimental results showing that the power spectrum of the ground-state vibrational modes of neat liquid THF may have a complex structure even in regions where no stationary absorption is expected. This investigation is enabled by our novel setup that can detect broadband ultrafast transient spectrum with single-delay-scan.

2. Experimental

The detailed experimental setup for pump–probe spectroscopy has been reported [17]. The output beam of a regenerative amplifier (Spitfire, Spectra Physics) was separated into two beams: One fraction was frequency-doubled and used as a pump for a noncollinear optical parametric amplifier (NOPA); the other was focused onto a sapphire plate to generate a white-light continuum, which was used as a seed for the NOPA. The output of the NOPA was used for the pump and probe pulses after including chirp compensation

* Corresponding author. Present address: Max-Planck-Institut für Quantenoptik, Hans-Kopfermann-Straße 1, 85748 Garching, Germany.
E-mail address: akira.ozawa@mpq.mpg.de (A. Ozawa).

0009-2614/$ - see front matter © 2009 Elsevier B.V. All rights reserved.
doi:10.1016/j.cplett.2009.06.098

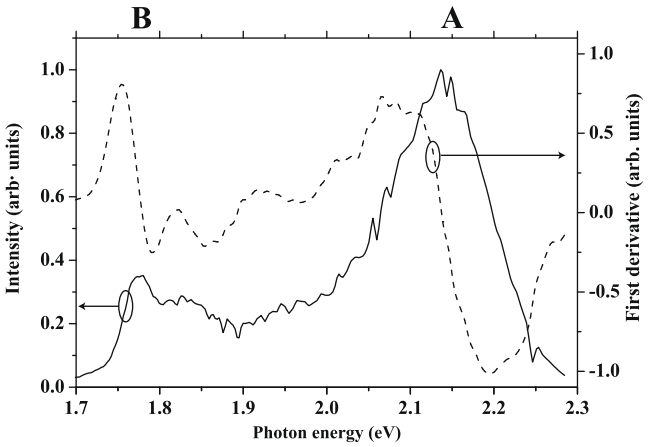

Fig. 1. Laser spectrum (solid line) and its first derivative (dashed line) after smoothing.

with a pair of chirped mirrors and prisms. Thus obtained laser spectrum after chirp compensation is shown in Fig. 1. The setup was optimized to obtain pump and probe energies as high as 40 and 6 nJ, respectively, for efficient ISRS excitation.

A liquid tetrahydrofuran (THF) sample (Kanto Chemicals) was taken in a cuvette of 1 mm thickness. The positive chirp induced at the cuvette window was pre-compensated by optimizing the prism compressor to give the shortest possible pulse inside the sample. All the experiments were performed at room temperature.

3. Results and discussion

3.1. Normalized transmittance change

With a home-developed multi-channel lock-in amplifier, the real-time traces were measured in the range of 1.68–2.28 eV. The experimental data represent two-dimensional plots of the normalized transmittance change ($\Delta T/T$) as a function of the probe photon energy and the probe delay time. Fig. 2 shows the resultant $\Delta T/T$ plots for the probe photon energies ranging from 1.70 to 2.15 eV. Modulation by molecular vibration is clearly observed around the zero-signal line. The modulation amplitude of $\Delta T/T$, $\sim 5 \times 10^{-3}$, corresponds to the change in the equivalent absorbance, ΔA, $\sim 2 \times 10^{-3}$.

In addition to the apparent vibrational mode with a period of 37 fs, higher-frequency vibration components with periods of ~12 fs were also identified. From a Fourier transform analysis of these real-time traces, the following modes were obtained: 911 ± 12, 2836 ± 11, 2880 ± 11, and 2924 ± 10 cm^{-1}. The last mode, 2924 cm^{-1}, is one of the highest frequencies observed in real time [6]. The higher-frequency modes seemed to fade out with a delay time as short as ~200 fs. This behavior can be ascribed partly to the interference among the high-frequency modes. The revival was observed at ~300 fs. By comparing with the results of Raman spectroscopy [18], the three modes with higher frequencies were assigned to the C–H stretching modes. The baseline of the $\Delta T/T$ signal up to ~150 fs deviates slightly from the zero-signal line. A possible mechanism is the libration of THF, as observed for CS_2 [19–22].

3.2. FFT power spectrum of the real-time trace

The real-time traces obtained at each probe photon energy level were Fourier transformed to obtain the vibrational fast Fourier transform power spectrum as a function of the probe photon energy. Fig. 3 shows the probe photon energy dependence of the Fourier power of the 2880 cm^{-1} mode. The spectrum contains two peaks at ~2.14 and ~1.78 eV. Since the laser spectrum shown in Fig. 1 lies in the visible region, far from the absorption band of the sample, the effects of electronic transition are negligible. Note that a plot of the vibrational power versus the probe photon energy is complicated and contains narrow peaks, even in a transparent medium without single-photon transition.

As reported in Ref. [8], the probe pulse can be modulated by a dynamic alternation of the refractive index caused by the ground-state vibrational wave packets produced by ISRS. If this is the case, the FFT spectrum should be reproduced by the first derivative of the laser spectrum under the approximation of small

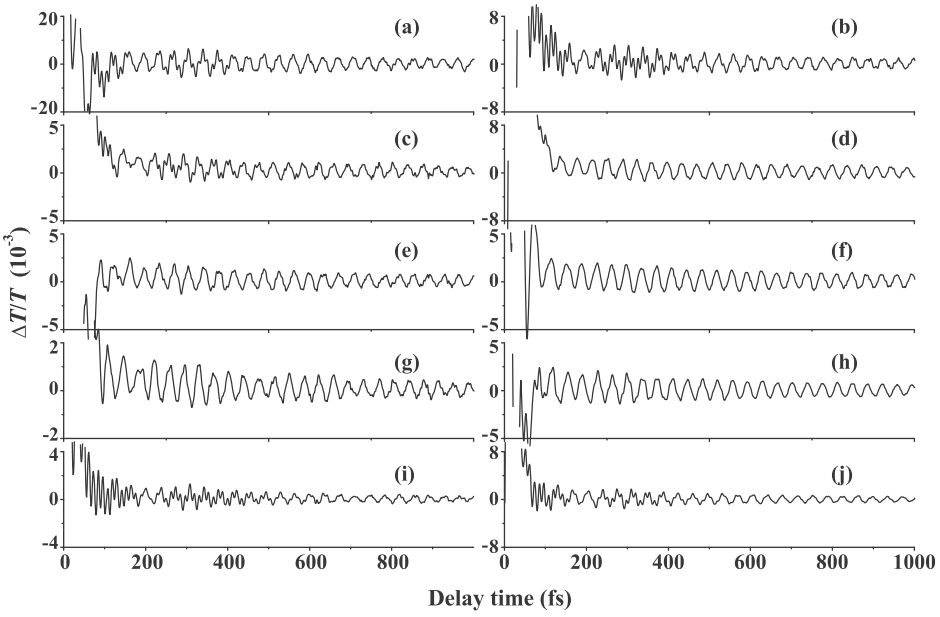

Fig. 2. Real-time traces of normalized transmittance change ($\Delta T/T$) for probe photon energies of (a) 1.70, (b) 1.75, (c) 1.80, (d) 1.85, (e) 1.90, (f) 1.95, (g) 2.00, (h) 2.05, (i) 2.10, and (j) 2.15 eV.

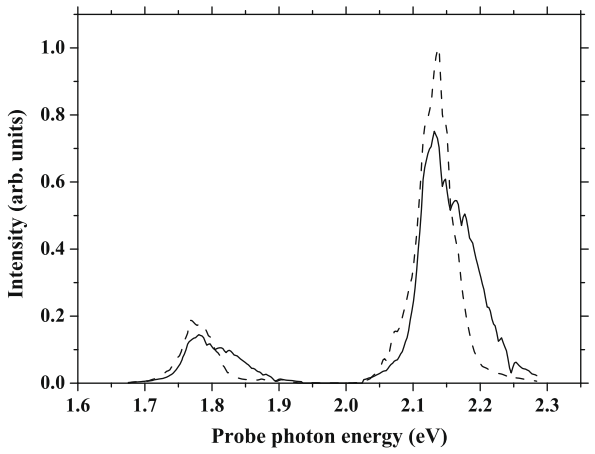

Fig. 3. Fourier power spectrum of the 2880 cm^{-1} mode (dashed line) and the fit to the model curve (solid line).

modulation. Fig. 1 shows the first derivative of the laser spectrum for comparison with the FFT power spectrum shown in Fig. 3. Since no essential correlation is observed between the two plots, the former model can hardly explain the observations.

In order to interpret this FFT spectrum, we propose the existence of dynamic coherent coupling through the Raman process between the fundamental field and the Stokes-shifted field due to ground-state molecular vibration. The Raman coupling under various conditions among the fundamental, Stokes, and anti-Stokes fields and molecular vibrational polarization has been studied theoretically and experimentally [23–25]. In the presence of vibrational polarization, energy transfer can occur between pairs of spectral components whose energy difference is equal to the vibration energy. The relative phase between the vibrational polarization and the laser field determines the direction of the energy transfer between the fundamental and the Stokes fields. In the pump–probe experiments, the delay time corresponds to the relative phase, because the ground-state vibration is induced impulsively by the pump pulse.

3.3. Modeling of the Raman process

For a further examination of this phenomenon, the following model is formulated: The general coupling equations of the fundamental (f), Stokes-shifted (s), and anti-Stokes-shifted (as) fields with the molecular vibrational polarization are given as

$$P_{\omega v} = \gamma Q, \tag{1a}$$

$$\left(\frac{\partial^2}{\partial t^2} + \omega_v^2\right) Q = a(E_f E_s^* + E_{as} E_f^*), \tag{1b}$$

$$P_{\omega f} = d_s E_s Q + d_{as} E_{as} Q^*, \tag{1c}$$

$$P_{\omega s} = d_s E_f Q^*, \tag{1d}$$

$$P_{\omega as} = d_{as} E_f Q, \tag{1e}$$

$$\nabla^2 E_m = \mu_0 \sigma \frac{\partial E_m}{\partial t} + \mu_0 \varepsilon_m \frac{\partial^2 E_m}{\partial t^2} + \mu_0 \frac{\partial^2 P_{\omega m}}{\partial t^2} \quad (m = f, s, as). \tag{1f}$$

Here, Q, E, and P indicate the relevant vibrational normal coordinates, electric field, and macroscopic polarization, respectively. The symbols d_m, a, and γ represent the proportional constants. The angular frequency of molecular vibration is denoted as ω_v. At the focal point in the sample, the plane-wave approximation for both the electric fields and the sinusoidal molecular vibration is applied as follows:

$$Q = Q_0 \exp(i(\omega_v t - \phi)), \tag{2a}$$

$$E_m = E_m(z) \exp(i(\omega_m t - k_m z)). \tag{2b}$$

Here, the relative phase between the molecular vibration and the laser field, denoted as ϕ, is proportional to the delay time between the pump pulse and the probe pulse. $E_m(z)$ represents the slow evolution of field intensity by the Raman-coupling process. Since the energy of the vibrational mode focused here is approximately equal to the laser spectrum bandwidth, the coupling of only the higher- and lower-energy spectral portions (the regions of A and B in Fig. 1, respectively) must be considered. In the present report, we denote the spectral regions corresponding to A and B as the fundamental field and the Stokes-shifted field, respectively.

Under the assumption of slowly varying envelope approximation, Eqs. (1) and (2) give the following coupling equations between the fundamental and Stokes fields, by neglecting the anti-Stokes field in the weak interaction limit, which is well satisfied in this experiment

$$\frac{\partial E_f(z)}{\partial z} = -\frac{i\mu_0 d_s Q_0 \omega_f^2}{2k_f} E_s(z) \exp(-i(k_s - k_f)z - i\phi), \tag{3a}$$

$$\frac{\partial E_s(z)}{\partial z} = -\frac{i\mu_0 d_s Q_0 \omega_s^2}{2k_s} E_f(z) \exp(i(k_s - k_f)z + i\phi), \tag{3b}$$

For simplicity, we investigate here the behavior for small z by expanding the solution of Eqs. (3) to the first order of z:

$$E_s(z)E_s(z)^* = E_{s0}^2 + \frac{z d_s k_s Q_0}{\varepsilon_s} E_{f0} E_{s0} \sin(-\phi), \tag{4a}$$

$$E_f(z)E_f(z)^* = E_{f0}^2 + \frac{z d_s k_f Q_0}{\varepsilon_f} E_{f0} E_{s0} \sin(\phi). \tag{4b}$$

In these expressions, E_{f0} and E_{s0} indicate the initial values of the electric fields: $E_{f0} \equiv E_f(z = 0)$ and $E_{s0} \equiv E_s(z = 0)$. The effect of phase mismatch is ignored.

Eqs. (4) show the sinusoidal modulation of the Stokes and fundamental fields when ϕ is scanned by changing the pump and probe pulse delay. It can also be seen that the modulation amplitude is expressed by the product of Stokes-shifted and fundamental field amplitudes. This is a direct consequence of Raman coupling, in which two photons of fundamental and Stokes fields both contribute to the process. Thus, in the absence of spectral overlap between the Stokes- and anti-Stokes-shifted laser spectra, the FFT power spectrum can be expressed by the product of the original laser spectrum and the shifted laser spectrum by the vibrational energy:

$$(\Delta T(\omega))_{\mathrm{FFTpower}} = \omega^2(\alpha^2 I(\omega) I(\omega - \omega_v) + \beta^2 I(\omega + \omega_v) I(\omega)), \tag{5}$$

where $I(\omega)$ is the laser intensity at the optical angular frequency ω, and α, β are free parameters.

3.4. Comparison with the experiment

The experimental FFT power spectrum is reproduced based on Eq. (5), and shown in Fig. 3. The two free parameters are adjusted to obtain the best-fit data. The agreement obtained both for the peak positions and the peak widths indicates that the proposed model is reasonable. The high- and low-energy peaks correspond to the fundamental and Stokes fields, respectively.

The initial phases of the modulations of the fundamental and Stokes-shifted field are expected to be shifted by π radians from each other, as can be seen by the negative and positive ϕ values appearing in the sine functions in Eqs. (4). The experimental initial phase of the mode of 2880 cm^{-1}, obtained by the FFT analysis, is shown in Fig. 4. This phase shows a clear π phase jump at 1.98 eV. This energy is located just between the fundamental and Stokes peaks of the FFT spectrum, which also supports our model. Similar phase features are also observed for other high-frequency modes at 2836 and 2924 cm^{-1}.

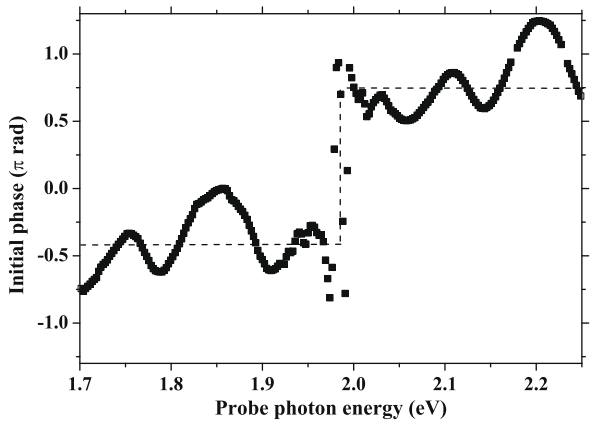

Fig. 4. Initial phase of the 2880 cm^{-1} mode. The dashed line is a guide for the eye.

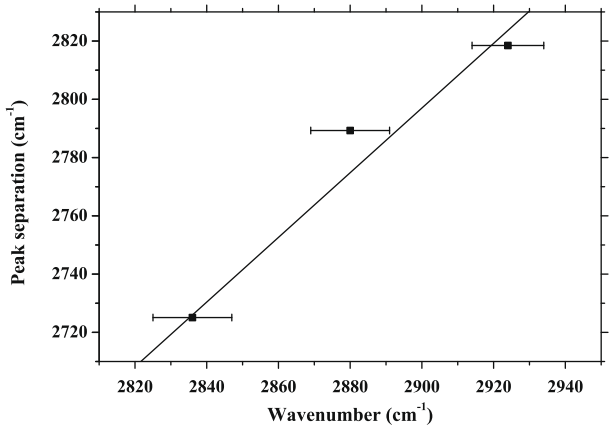

Fig. 5. Energy difference between two peaks in the FFT power spectrum as a function of the mode wavenumber.

As expected from Eq. (5), the energy difference between the two peaks of the FFT power spectrum increases with the vibrational energy. In order to study this property for the three observed modes, the energy difference between the two peaks of the FFT spectrum was calculated. As shown in Fig. 5, the energy difference clearly increased. The plot fitted with a linear function gave a gradient of 1.1 ± 0.2, which is close to the expected value of 1.

These evidences, gained from the fitting of the FFT power spectrum, the initial phase and the FFT spectral shift, lead to the conclusion that the observed higher-frequency modulation is due to the dynamic coupling between the two spectral components in the probe pulse through molecular vibrations of the ground state. This process is versatile, as it is also expected in the pump–probe experiments with resonant electronic transition. The modulation observed in the spectral region remote from that of stationary absorption has been often assigned to excited-state molecular vibration. It is revealed that the Raman process can also produce complex structures of vibrational amplitude in the spectral region without absorption, which may have been misinterpreted as contributions from excited-state molecular vibrations.

4. Conclusion

The transparent neat liquid of THF was investigated by sub-5-fs time-resolved absorption spectroscopy. Intensity modulation of the transmitted probe pulse was observed, and its FFT power was obtained as a function of the probe photon energy. It was revealed both experimentally and theoretically that the vibrational FFT power spectrum may have peak structures even in the optically transparent spectral region without electronic transitions.

This observation is explained by the Raman process, which couples the two spectral components of the driving laser that are separated by the energy of molecular vibration. These results suggest the possibility that the constitution of the ISRS process is confused with those of excited-state wave packets in conventional interpretations of pump–probe experiments. The present study gives warning that a careful study is needed in the interpretation of vibrational components in transient absorption spectroscopy.

Acknowledgements

The authors are grateful to Dr. F. Araoka and Dr. S. Adachi for their careful reading of the manuscript. This research is supported partly by a Grant-in-Aid for Specially Promoted Research (#14002003) from the Ministry of Education, Culture, Sports, Science and Technology (MEXT) and partly by the program for the 'Promotion of Leading Researches' in Special Coordination Funds for Promoting Science and Technology from MEXT.

References

[1] T. Kobayashi, T. Saito, H. Ohtani, Nature 414 (2001) 531.
[2] G. Cerullo, D. Polli, G. Lanzani, S. De Silvestri, H. Hashimoto, R.J. Cogdell, Science 298 (2002) 2395.
[3] Y. Yuasa, M. Ikuta, T. Kobayashi, T. Kimura, H. Matsuda, Phys. Rev. B 72 (2005) 134302.
[4] J.S. Melinger, V.D. Kleiman, D. McMorrow, F. Grohn, B.J. Bauer, E. Amis, J. Phys. Chem. A107 (2003) 3424.
[5] V.D. Kleiman, J.S. Melinger, D. McMorrow, J. Phys. Chem. B105 (2001) 5595.
[6] D. Polli, L. Lüer, G. Cerullo, Rev. Sci. Instrum. 78 (2007) 103108.
[7] Y.-X. Yan, E.B. Gamble Jr., K.A. Nelson, J. Chem. Phys. 83 (1985) 5391.
[8] P.J. Rizo, T. Kobayashi, App. Phys. Lett. 85 (2004) 28.
[9] N. Ishii, E. Tokunaga, S. Adachi, T. Kimura, H. Matsuda, T. Kobayashi, Phys. Rev. A 70 (2004) 023811.
[10] O. Steinkellner, M. Wittmann, G. Korn, I.V. Hertel, App. Phys. B 73 (2001) 279.
[11] R. Ruhman, A.G. Joly, K.A. Nelson, J. Chem. Phys. 86 (1987) 6563.
[12] I.A. Walmsley, F.W. Wise, C.L. Tang, Chem. Phys. Lett. 154 (1989) 315.
[13] J.K. Wahlstrand, R. Merlin, X. Li, S.T. Cundiff, O.E. Martinez, Opt. Lett. 30 (2005) 926.
[14] Y.R. Shen, N. Bloembergen, Phys. Rev. 137 (1965) A1787.
[15] M. Ikuta, Y. Yuasa, T. Kimura, H. Matsuda, T. Kobayashi, Phys. Rev. B 70 (2004) 214301.
[16] A.T.N. Kumar, F. Rosca, A. Widom, M. Champion, J. Chem. Phys. 114 (2001) 701.
[17] A. Shirakawa, I. Sakane, M. Takasaka, T. Kobayashi, App. Phys. Lett. 74 (1999) 2268.
[18] G. Echhardt, IEEE. J. Quant. Electr. 2 (1966) 1.
[19] T. Hattori, T. Kobayashi, J. Chem. Phys. 94 (1991) 3332.
[20] T. Hattori, A. Terasaki, T. Kobayashi, T. Wada, A. Yamada, H. Sasabe, J. Chem. Phys. 95 (1991) 937.
[21] D. McMorrow, W.T. Lotshaw, G.A. Kenny-Wallace, IEEE J. Quant. Electr. QE24 (1988) 443.
[22] S. Ruhman, B. Kohler, A.G. Joly, K.A. Nelson, Chem. Phys. Lett. 141 (1987) 16.
[23] G.P. Djotyan, J.S. Bakos, J. Mod. Opt. 41 (1994) 1687.
[24] S.M. George, C.B. Harris, Phys. Rev. A 28 (1983) 863.
[25] S. Constantine, Y. Zhou, J. Morais, L.D. Ziegler, J. Phys. Chem. A 101 (1997) 5456.